Journal of Inorganic and General Chemistry
ZAAC
Zeitschrift für anorganische und allgemeine Chemie
www.zaac.wiley-vch.de
RESEARCH ARTICLE
DOI: 10.1002/zaac.202200349

Novel Homoleptic and Heteroleptic Pt(II) β-oxodithiocinnamic ester Complexes: Synthesis, Characterization, Interactions with 9-methylguanine and Antiproliferative Activity

Micheal K. Farh,[a, b] Norman Häfner,[c] Helmar Görls,[a] Ingo B. Runnebaum,*[c] and Wolfgang Weigand*[a, d]

Three new series of homoleptic and heteroleptic platinum(II) β-oxodithiocinnamic ester complexes, [Pt(L1–L9)$_2$], [Pt(L1–L9)(DMS)Cl] and [Pt(L1–L9)(DMSO)Cl], were synthesized and characterized using elemental analysis, mass spectrometry, and different NMR spectroscopy (^{1}H, ^{13}C{^{1}H} and ^{195}Pt). The β-oxodithiocinnamic esters coordinate towards the platinum(II) centre as O,S-bidentate chelating ligands. The structures of HL3, [Pt(L2)$_2$], [Pt(L6)(DMS)Cl] as well as [Pt(L2)(DMSO)Cl] have been confirmed through the X-ray crystallography, where the platinum(II) complexes exhibit a slightly distorted square planar geometry. In this article, we also investigated the solvolysis of three representative Pt(II) complexes, as well as the interaction with 9-methylguanine as a DNA model system, by utilizing the LC-ESI-MS technique. A selection of the complexes was assessed for their use as anticancer agents, and cytotoxicity assays with these complexes showed modest toxicity on both Cisplatin sensitive and resistant ovarian cancer cell lines. However, the compounds cytotoxicity was not affected by the Cisplatin resistance mechanisms and a specific selection of the ligands may modify the cell line specificity.

Introduction

β-oxodithioesters are highly efficient intermediates in organic synthesis, and despite their differing reactivities, considered parallel synthons for β-ketoester chemistry.[1–7] Also, they exhibit keto-enol tautomerism (Figure 1), which is shifted towards the enol form due to the high electronegativity of the β-keto group that makes the α-protons more acidic.[1] The enol form is also stabilized by the intramolecular hydrogen bonding and the conjugated system (Figure 1A).[1] Furthermore, β-oxodithioesters contain polyfunctional groups with multi-reactive centers including three nucleophilic and two electrophilic centers, as shown in (Figure 1B and 1C). Synthons containing both electrophilic and nucleophilic centers have significant potential for developing more effective reaction pathways during the construction of various heterocyclic systems.[1–4] As a result of those active centers and the specific advantages of easy preparation and versatile reactivity, β-oxodithioesters have been widely applied as a valuable building block in the synthesis of several organosulfur moieties, in which sulfur acts either as an internal or external substituent.[1–7] In addition, β-oxodithioesters have been employed as O,S-chelating ligands in the synthesis of several homo and heteroleptic transition metal complexes.[8–16] Several zinc(II), cadmium (II), nickel(II), and copper (II) β-oxodithioester complexes have been reported by

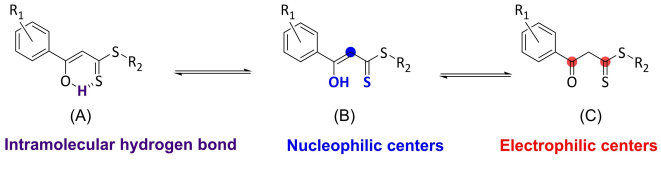

Figure 1. Structure of β-hydroxydithiocinnamic ester derivatives (intramolecular hydrogen bond, and active sites).

[a] M. K. Farh, H. Görls, W. Weigand
Institut für Anorganische und Analytische Chemie,
Friedrich-Schiller-Universität,
Humboldtstraße 8,
07743 Jena, Germany
E-mail: wolfgang.weigand@uni-jena.de
[b] M. K. Farh
Department of Chemistry,
Faculty of Science,
Assiut University
Assiut 71515, Egypt
[c] N. Häfner, I. B. Runnebaum
Department of Gynecology,
Jena University Hospital – Friedrich Schiller University Jena,
Am Klinikum 1,
07747 Jena, Germany
E-mail: Direktion-Gyn@med.uni-jena.de
[d] W. Weigand
Jena Center for Soft Matter (JCSM),
Friedrich Schiller University,
Philosophenweg 7,
07743 Jena, Germany

Supporting information for this article is available on the WWW under https://doi.org/10.1002/zaac.202200349

Singh and co-workers to catalyze the transformation of many organic reactions.[8–10] Moreover, some nickel(II), palladium(II), and platinum(II) β-oxodithioester complexes exhibited antileishmanial activities.[11] A series of nickel(II), palladium(II), platinum(II), ruthenium(II), and osmium(II) β-oxodithioester complexes have been also reported by Weigand and co-workers to possess anticancer activities.[12–17] It is worth mentioning that the co-operative effects of electronic and geometric properties in metal-organic ligand structures ultimately promote highly diverse interactions with biological targets, providing opportunities for drug activity and development.[12–18] Although Cisplatin is one of the most effective cancer drugs,[19–25] there is a significant adverse effect on normal cells and tissues, cross-resistance, and severe side effects that make it critical to find new platinum-based drugs with a manageable set of side effects applicable for clinical use.[26–28]

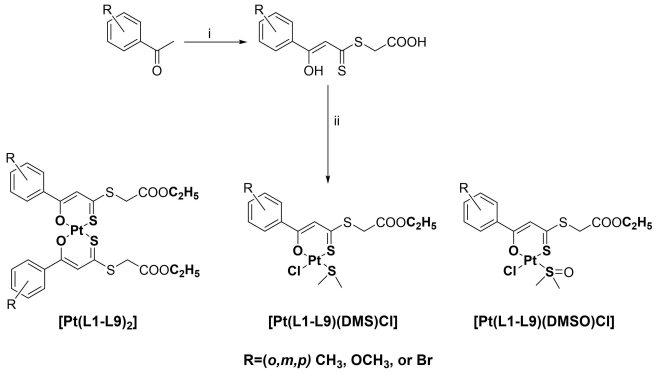

Scheme 1. Synthesis of β-hydroxydithiocinnamic ester ligands HL1-HL9 and their corresponding complexes $[Pt(L1–L9)_2]$, [Pt(L1–L9)(DMS)Cl], and [Pt(L1–L9)(DMSO)Cl]: i, KO^{t}Bu (2 eq.), diethyl ether (40 mL), −78 °C, 2-bromoacetic acid (1 eq.), r.t.; ii, $[PtCl_2(DMS)(DMSO)]$ (1 eq.), ethanol (40 mL), 60 °C 30 min., overnight r.t.

Results and Discussion

Several advanced methods have been developed for the synthesis of β-oxodithioesters. Thuillier *et al.* utilize enolizable ketones as acetophenone derivatives that, when treated with a strong base, generate active methylene compounds, which further react with CS_2 to provide the sodium salt of dithiocarboxylic acid that can be alkylated to the respective β-oxodithioesters.[29] Another convenient method was described by Junjappa and co-workers, in which the active methylene ketones were treated with (S,S)-dimethyl trithiocarbonate in a DMF-hexane mixture affording the desired β-oxodithioesters.[30] Alternatively, Junjappa *et al.* by using 3-methylimidazolium-1-carbodithioic acid methyl ester instead of (S,S)-dimethyl trithiocarbonate with active methylene compounds, β-oxodithioesters can be also obtained.[31] β-hydroxydithiocinnamic esters used in this study were prepared according to the Thuillier method with some modifications. The acetophenone derivatives were first treated with potassium tert-butoxide and then carbon disulfide to obtain the sodium salt of dithiocarboxylic acid that can be reacted in situ with 2-bromoacetic acid instead of the normal alkyl halide as established in the previous synthetic methods, affording finally the new class of β-hydroxydithiocinnamic ligands (Scheme 1). These ligands show some interesting features: (i) O,S-bidentate chelating ligand, (ii) keto-enol tautomerism (iii) having both hard oxygen and soft sulfur donor atoms, (iv) different functional groups on the benzene ring and terminal carboxylic group which may influence the electronic and steric properties. Based on these features as well as the remarkable stability of such kind of platinum(II) β-hydroxydithiocinnamic complexes in both pure DMSO and DMSO-buffer solutions reported previously by our group,[13–15] we now present the synthesis of the platinum(II) β-hydroxydithiocinnamic ester complexes using the platinum(II) precursor complex *cis*-$[PtCl_2(DMS)(DMSO)]$. *Cis*-$[PtCl_2(DMS)(DMSO)]$ was prepared according to the previous literature procedure[32] and reacts with the β-hydroxydithiocinnamic ester ligands in ethanolic solution to generate the desired platinum(II) complexes (Scheme 1). Three different classes of compounds were obtained through this method: homoleptic bis-chelate complexes $[Pt(L1–L9)_2]$ and two heteroleptic mono-chelate complexes with dimethyl sulfide [Pt(L1–L9)(DMS)Cl] or dimethyl sulfoxide [Pt(L1–L9)(DMSO)Cl] and one chloride ligand (Scheme 1). It is also noteworthy that the terminal carboxylic group was esterified during the coordination, as indicated by X-ray structure analysis, NMR spectroscopy and mass spectrometry. The bonding of the soft platinum(II) ions towards soft (S) and hard (O and Cl^-) donors are based on antisymbiosis and HSAB principles, where each two sulfur donors are coordinated *cis* to each other, while *trans* to hard donors (O or Cl^-).[33,34] This coordination may make significant differences in the stability of Pt–Cl, Pt–O, and Pt–S bond polarity and hence the reactivity of the complexes.

Spectroscopic characterization

All compounds were characterized by NMR spectroscopy, mass spectrometry and elemental analysis. The chemical shifts in ^{1}H NMR and ^{13}C{1H} NMR spectra for ligands HL1-HL9 are generally in good agreement with previously reported values.[8–17,35–39] In the ^{1}H NMR spectra, HL1-HL9 display a single resonance signal in the range of δ 14.49–15.17 ppm belonging to the hydroxyl group (–OH) proton, which is not observed in the complexes $[Pt(L1–L9)_2]$, [Pt(L1–L9)(DMS)Cl], and [Pt(L1–L9)(DMSO)Cl]. The methine proton (=CH–) found at δ 6.66–7.44 ppm and δ 6.76–7.32 ppm for the ligands and complexes, respectively, is virtually unchanged. A single resonance signal at δ 11.40–13.07 ppm corresponding to the (–COOH) proton of the free ligands HL1-HL9 is disappeared in the ^{1}H NMR spectra of the complexes $[Pt(L1–L9)_2]$, [Pt(L1–L9)(DMS)Cl], and [Pt(L1–L9)(DMSO)Cl]. Furthermore, the appearance of additional signals at δ 1.30 ppm (triplet) and δ 4.24 ppm (quartet) in the ^{1}H NMR spectra of the complexes and a downfield shift of around 0.23 and 0.5 ppm, respectively, compared to ethanol signals, confirm

the esterification of the carboxylic group during the coordination of the ligands.[40] In the $^{13}C\{^1H\}$ NMR spectra, resonances for the (C–OH) carbon were found in the range of δ 168.91–174.11 and δ 171.52–177.35 ppm, for the ligands and complexes, respectively. The methine (=CH–) carbon of the free ligands found in the range of δ 106.64–111.22 ppm is slightly downfield shifted by ≈5 ppm in the complexes to δ 111.53–116.71 ppm, because of the slightly deshielding effect through the delocalization of the electrons in the chelating ring.[13–16] In contrast, a considerable upfield shift is observed for the quaternary thiocarbonyl carbon (C=S) at δ 174.27–180.47 ppm in the complexes, compared to the free ligands (δ 213.50–216.37 ppm). As a result of coordinating β-hydroxydithiocinnamic esters to the platinum(II) center, the β-oxo carbon atom is deshielded, while the thiocarbonyl group accepts the π-backbonding electron density from the platinum(II) center and thus shields the thiocarbonyl carbon atom.[8–17] [Pt(L1–L9)(DMS)Cl] complexes exhibit a characteristic signal for the coordinated dimethyl sulfide (DMS) in both ^1H and $^{13}C\{1H\}$ NMR spectra. The methyl groups were found at δ 2.60 ppm as a singlet with platinum satellites $^3J_{Pt-H}$ ≈ 50 Hz in the ^1H NMR spectra and δ 24 ppm with platinum–carbon coupling $^2J_{Pt-C}$ ≈ 18 Hz in the $^{13}C\{^1H\}$ NMR spectra. Also, there is a downfield shift by 0.5 and 6 ppm compared to free DMS in both ^1H and $^{13}C\{1H\}$ NMR spectra, respectively.[41] The methyl groups of the coordinated dimethyl sulfoxide (DMSO) in [Pt(L1–L9)(DMSO)Cl] complexes were observed at δ 3.60 ppm as a singlet accompanied by platinum satellites $^3J_{Pt-H}$ ≈ 22 Hz in the ^1H NMR spectra and δ 46 ppm with platinum–carbon coupling $^2J_{Pt-C}$ ≈ 50 Hz in the $^{13}C\{1H\}$ NMR spectra, respectively. Compared to the free DMSO, there is observed a downfield shift by 1.1 and 6 ppm in both ^1H and $^{13}C\{1H\}$ NMR spectra, respectively, which also confirm the formation of a mono-chelate complex with S-coordinated DMSO ligand which is in accordance with previously described Pt-DMSO complexes.[13–16,35–39,42–46] ^{195}Pt NMR spectra for the bis-chelate complexes [Pt(L1–L9)$_2$] as well as the mono-chelate complexes [Pt(L1–L9)(DMS)Cl] and [Pt(L1–L9)(DMSO)Cl] were obtained. The signals appeared in the range of (−2267 to −2350 ppm) and (−2879 to −3079 ppm), for the bis-chelate and mono-chelate complexes, respectively, which is in good agreement with the previously reported values.[42–46]

Molecular structures

Recrystallization from a mixture of CH_2Cl_2 and cyclohexane (1 : 1) of [Pt(L2)$_2$], [Pt(L2)(DMSO)Cl] and [Pt(L6)(DMS)Cl] complexes as well as HL3 ligand at 20 °C produced suitable single crystals for X-ray diffraction studies. Molecular structures are provided in Figure 2 with ellipsoids drawn at the 50 % probability level. Crystallographic data as well as structure solution and refinement details are summarized in Table S1. Selected bond lengths and angles are given in Table S2. The platinum(II) metal centers in each of the platinum(II) complexes is found in a slightly distorted square-planar coordination mode. In the case of complexes [Pt(L2)(DMSO)Cl] and [Pt(L6)(DMS)Cl], the sulfur atoms (S3) of the DMSO or DMS moiety are coordinated *cis* to

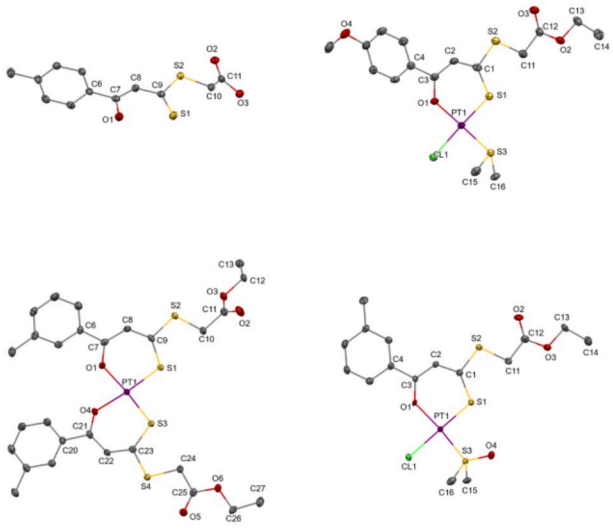

Figure 2. Depiction of solid-state molecular structures of HL3 (top-left), [Pt(L2)$_2$] (down-left), [Pt(L6)(DMS)Cl] (top-right) and [Pt-(L2)(DMSO)Cl] (down-right). Thermal ellipsoids are given at the 50 % probability level and hydrogen atoms are omitted for clarity.

the sulfur atom (S1) of the O,S bidentate ligand, while *trans* to each of the soft sulfur atom is located a hard donor atom (O1 or Cl^-). The bond lengths of platinum and their donor atoms are decreasing as following: Pt–Cl > Pt–S1 ≈ Pt–S3 > Pt–O1. Moreover, [Pt(L2)(DMSO)Cl] coordination sphere angles comes close to 90° for S1–Pt–S3 (89.81(3)°) and S3–Pt–Cl (89.60(3)°), is smaller for O1–Pt–Cl (84.42(7)°) and larger in the case of O1–Pt–S1 (96.17(7)°). Meanwhile, the angles in the coordination sphere of [Pt(L6)(DMS)Cl] are higher than 90° for O1–Pt–S1 (96.74(9)° and S3–Pt–Cl (93.49(4)°), and smaller for O1–Pt–Cl (85.65(9)°) and S1–Pt–S3 (84.12(4)°). Upon coordination, the chelating ligand also undergoes structural changes, the C3–O1 bond is significantly shorter, while the C1–S1 bond is elongated, reflecting an increasing double-bond character for the C–O bond and an increasing single-bond character for the C–S bond. Additionally, all carbon-carbon bonds and carbon skeleton angles in the 6-membered chelating ring are almost equal, which confirms a good delocalization of electron density there. This behavior agrees with the $^{13}C\{^1H\}$ NMR data obtained for both complexes. The chelating unit's angles are widened to achieve square-planar coordination towards the platinum center. The angle Pt–O1–C3 is the widest (131.9(2)° in [Pt-(L2)(DMSO)Cl] and 129.5(5)° in [Pt(L6)(DMS)Cl]) whereas, the Pt-S1-C1 angle is the smallest (107.55(12)° in [Pt(L2)(DMSO)Cl] and 108.90(14)° in [Pt(L6)(DMS)Cl]). The bis-chelate complex [Pt(L2)$_2$] is almost identical to those of the corresponding mono-chelated species, with the only difference being non-existent of DMS or DMSO ligands. The two ligands are *cis* coordinated, as reported earlier for analogous structures.[13–16] The angles of the coordination sphere are larger than 90° for O1–Pt–S1 (95.68(6)°), and O4–Pt–S3 (95.94(6)°), close to 90° for S1–Pt–S3 (89.50(3)°) and therefore smaller than 90° for O1–Pt–O4

(76.90(8)°). The chelating units are planar with slightly widened angles, as it was observed for [Pt(L2)(DMSO)Cl] and [Pt-(L6)(DMS)Cl] complexes.

Stability and solvolysis of the Pt(II) complexes

The solvolysis of three representative Pt(II) complexes [Pt(L6)$_2$], [Pt(L6)(DMS)Cl], and [Pt(L6)(DMSO)Cl] in CH_3CN-PBS (pH 7.4; 1:1) at 37 °C for 72 hours was monitored by LC-ESI-MS spectroscopy (positive ion mode) (Figure S1–S3). The ESI spectra of the [Pt(L6)(DMS)Cl], and [Pt(L6)(DMSO)Cl] complexes clearly show a peak at *m/z* = 587.6 assigned to $[(Pt(L6)(CH_3CN)_2]^+\cdot$ (t_R = 9.48 min, Figure S2 and S3), implying the efficient replacement of the chloride, DMS, or DMSO ligands. In the ESI spectrum of the [Pt(L6)(DMS)Cl] complex, an additional peak at *m/z* = 608.6 was observed and assigned to the $[(Pt(L6)(DMS)(CH_3CN)]^+\cdot$ (t_R = 9.6 min, Figure S2), demonstrating that only the Pt–Cl bond undergoes solvolysis, thus affording the mono-solvolysis species. Whereas the ESI spectrum of [Pt(L6)$_2$] complex shows a peak at *m/z* = 817.6 (t_R = 15.99 min, Figure S1), corresponding to the non-solvolysed complex and a less abundant peak at *m/z* = 587.7 (t_R = 9.48 min, Figure S1) was also observed. As shown in Figures S1–S3, there is no significant change in the spectral composition over time (24, 48 and 72 h). Based on these findings, the O,S–Pt(II) chelate units are stable under the study conditions, while the chloride, DMS, and DMSO ligands undergo solvolysis.

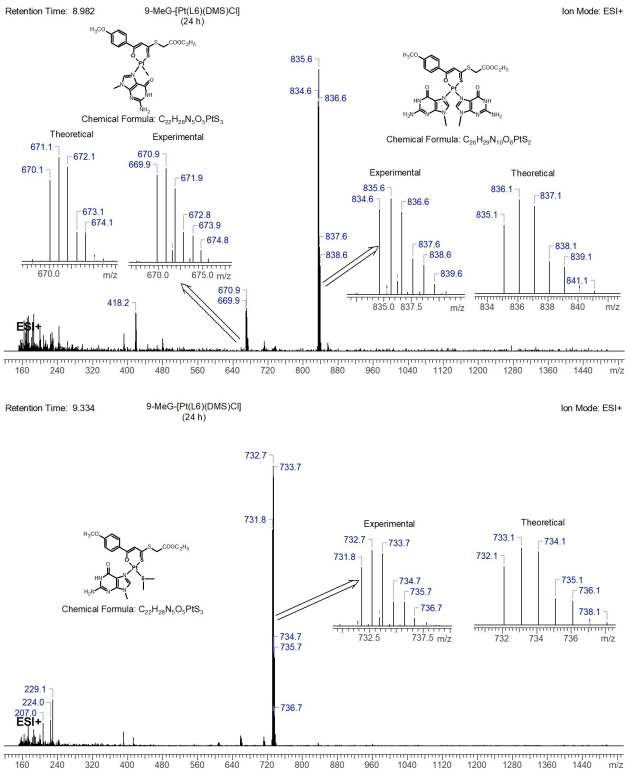

Figure 3. ESI-MS spectra of the adducts formed between 9-MeG and [Pt(L6)(DMS)Cl] complex after incubation 24 h at 37 °C. The insets show the theoretical as well as the experimental isotope patterns of *m/z* = 835.6 (t_R = 8.98 min), 732.7 (t_R = 9.33 min), and 670.9 (t_R = 8.98 min).

Interactions of the Pt(II) complexes with 9-methylguanine

As part of Cisplatin's mechanism of action, one or both chloride ligands are replaced by water molecules, thereby producing the potent electrophilic cations *cis*-$[Pt(NH_3)_2Cl(H_2O)]^+$ and *cis*-$[Pt(NH_3)_2(H_2O)_2]^{2+}$.[47–49] Afterwards, the aquated species can enter the nucleus, and the water molecule substituted by nucleophilic centers on DNA-purine bases, particularly the N7 positions of guanosine and adenosine residues.[47–49] In order to investigate the reaction of the synthetized Pt(II) complexes with 9-methylguanine (9-MeG) as a DNA model the representative Pt(II) complexes [Pt(L6)$_2$], [Pt(L6)(DMS)Cl], and [Pt(L6)(DMSO)Cl] (1 eq.) were incubated with 9-MeG (8 eq.) in CH_3CN-PBS (pH 7.4; 1:1) at 37 °C for 72 hours. The reaction was monitored by LC-ESI-MS (positive ion mode) to identify the formed Pt/9-MeG adducts (Figure 3, S4–S6). Upon reaction of the [Pt(L6)(DMS)Cl] complex with 9-MeG, two major peaks at *m/z* = 835.6 (t_R = 8.98 min), and 732.7 (t_R = 9.33 min) were found, assignable to the bifunctional adduct $[Pt(L6)(9\text{-MeG})_2]^+$ and the monofunctional adduct $[Pt(L6)(DMS)(9\text{-MeG})]^+$, respectively (Figure 3 and S5). In addition, a minor peak at *m/z* = 670.9 (t_R = 8.98 min) was observed and can be assigned to the N7,O6-bidentae 9-MeG adduct $[Pt(L6)(N7,O6\text{-}9\text{-MeG})]^+$, (Figure 3, and S5). In the ESI spectrum of the reaction between [Pt(L6)(DMSO)Cl] complex and 9-MeG, the main peak was found at *m/z* = 835.6 (t_R = 8.98 min), which can be assigned to the bifunctional adduct $[Pt(L6)(9\text{-MeG})_2]^+$. However, the minor peak at *m/z* = 670.8 (t_R = 8.98 min) assignable to $[Pt(L6)(N7,O6\text{-}9\text{-MeG})]^+$ adduct was also detected (Figure S6). Interestingly, the absence of any peaks attributed to [Pt(L6)(DMS)Cl], and [Pt(L6)(DMSO)Cl] complexes after 24 h indicates that the substitution reaction was completed. Also, there are no significant changes in spectral composition over time (24, 48 and 72 h) (Figure S5 and S6). In contrast, the ESI spectrum of [Pt(L6)$_2$] complex with 9-MeG, shows a major peak at *m/z* = 817.6 (t_R = 15.99 min), corresponding to the non-reacted complex as well as a minor peak at *m/z* = 835.6 (t_R = 8.98 min, Figure S4) assigned to the bifunctional adduct $[Pt(L6)(9\text{-MeG})_2]^+$. In agreement with its non-solvolytic behavior, this bis-chelate complex also exhibited the lowest 9-MeG binding. According to this study, such complexes, especially the heteroleptic mono-chelate complexes [Pt(L1–L9)(DMS)Cl] and [Pt(L1–L9)(DMSO)Cl] are capable of binding DNA-purine bases as well as forming stable mono- and bifunctional adducts.

Cytotoxic activity

The activity against the epithelial ovarian cancer cell lines A2780 and Skov3 and their Cisplatin-resistant subcultures was determined after 48 h incubation with varying concentrations of the compounds by the MTT assay as described before,[15] (see

Table 1. Mean IC50 values of the tested compounds and calculated resistance factors (RF) for A278 and Skov3 (for mean IC50 values with standard deviation, see supplementary data Tab. S3).

		A2780	A2780 Cis	RF A2780	Skov3	Skov3 Cis	RF Skov3	mean IC_{50}
DMS	L1	33.3	16.0	0.5	76.1	46.2	0.6	34.4
	L2	2056.6	355.0	0.2	685.8	183.1	0.3	656.1
	L3	56.1	60.5	1.1	57.5	41.4	0.7	43.3
	L4	55.0	72.2	1.3	60.6	53.2	0.9	48.5
	L5	93.0	59.1	0.6	119.9	69.6	0.6	68.4
	L6	59.5	46.4	0.8	86.6	69.7	0.8	52.6
	L7	28.1	44.7	1.6	63.9	53.7	0.8	38.4
	L8	42.6	50.7	1.2	66.3	63.7	1.0	44.9
	L9	32.9	39.4	1.2	60.6	52.6	0.9	37.3
DMSO	L1	25.6	55.3	2.2	336.8	99.4	0.3	103.8
	L2	164.4	50.4	0.3	380.9	103.6	0.3	139.9
	L3	n.a.						
	L4	16.5	73.3	4.5	146.1	92.8	0.6	66.6
	L5	224.6	58.5	0.3	777.3	95.5	0.1	231.2
	L6	n.a.						
	L7	102.8	56.3	0.5	646.9	182.8	0.3	197.9
	L8	64.6	48.2	0.7	87.6	54.9	0.6	51.2
	L9	153.8	76.8	0.5	403.9	163.6	0.4	159.7
CIS		6.8	15.4	2.3	12.5	28.6	2.3	13.1

the experimental section). The tested complexes [Pt(L1–L9)(DMS)Cl] and [Pt(L1, L2, L4, L5, and L7–L9)(DMSO)Cl], did not exhibit high cytotoxic activity and showed IC_{50} values higher than 16.0 μM (Table 1). Moreover, for several compounds, the calculated IC_{50} values are outside the range of analyzed concentrations (> 100 μM). Therefore, these compounds should be evaluated as ineffective. This is mainly the case for the Cisplatin-sensitive but not resistant cell lines. The analysis of higher concentrations was not compatible with the requirement of low solvent concentrations (< 0.5 % DMSO) for cell culture experiments.[15] Most compounds affected both sensitive and Cisplatin-resistant cells similarly or showed a higher activity against resistant cells resulting in resistance factors ($RF = IC_{50,resistant}/IC_{50,\ sensitive}$) $RF \leq 1$. These results are in agreement to earlier data of platinum(II) complexes with β-hydroxydithiocinnamic acid derivatives as O,S-chelating ligands.[15] Moreover, structure-activity relationships (SAR) can be revealed by the data and this may improve the design of future, more active organo-metal-based compounds. DMS and DMSO containing compounds have a similar mean activity (mean IC_{50} 132 μM and 135 μM, respectively) but exhibit cell line specific differences. Whereas DMS compounds are less cytotoxic for A2780 than for SKOV3 (mean IC_{50} 212 μM and 118 μM) the opposite is detected for DSMO compounds (mean IC_{50} 84 μM and 255 μM, respectively). Thus, cell line specific detoxification, DNA damage repair or cell death signaling processes influencing the cytotoxic activity may affect the two compound groups differently.

The comparison of compounds differing (i) in the position of the substituent (R) at the benzyl ring (meta; para; ortho position) or (ii) in the substituent itself ($-CH_3$; $-OCH_3$; $-Br$) did not reveal any general relationship to the cytotoxic activity. Again, DMS and DMSO-containing compounds differed regarding the substance group with the lowest activity (meta and para orientation for DMS and DMSO compounds, respectively; Figure 4). In agreement with earlier observations, the activity of such kind of platinum(II) β-hydroxydithiocinnamic acid complexes increases with increasing the lipophilicity of the terminal S-alkyl chain.[15] Therefore, the herein-presented compounds with the terminal hydroneutral ester group ($S{-}CH_2COOC_2H_5$) are less active than the previously reported platinum(II) complexes containing higher lipophilic β-hydroxydithiocinnamic acid derivatives.[15]

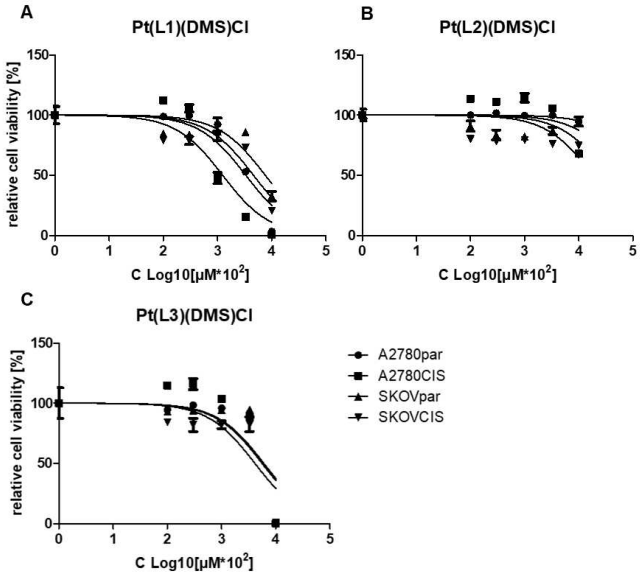

Figure 4. Exemplary data for the IC_{50} determination of the [Pt(L1–L3)(DMS)Cl] compounds with ortho-(A), meta-(B), or para-(C) substituent methyl group, respectively.

Conclusions

Here we reported on the synthesis of nine novel β-hydroxydithiocinnamic ester ligands HL1–HL9, that coordinated to the platinum(II) center of the precursor complex *cis*-[$PtCl_2$(DMS)(DMSO)] affording overall 27 platinum(II) complexes. Among them nine homoleptic bis-chelate complexes [Pt(L1–L9)$_2$], where two β-hydroxydithiocinnamic ester ligands coordinated *cis* to each other and 18 heteroleptic mono-chelate complexes with dimethyl sulfide [Pt(L1–L9)(DMS)Cl], or dimethyl sulfoxide [Pt(L1–L9)(DMSO)Cl] and chloride co-ligands. Structure determination was conceivable for the HL3 ligand as well as the platinum(II) complexes [Pt(L2)$_2$], [Pt(L2)(DMSO)Cl] and [Pt-(L6)(DMS)Cl]. A slightly distorted square-planar coordination mode was found in all the platinum(II) complexes. In the solvolysis experiment of the [Pt(L6)(DMSO)Cl] complex, both chlorido and DMSO ligands were rapidly replaced by two CH_3CN molecules, affording only the bi-solvolysis species [(Pt-(L6)(CH_3CN)$_2$]$^+$. The interaction of this complex with 9-MeG resulted in the formation of the bi-functional adduct [Pt(L6)(9-MeG)$_2$]$^+$, and also the N7,O6-bi-dentate 9-MeG adduct [Pt-(L6)(N7,O6-9-MeG)]$^+$ was observed. Alternatively, the solvolysis of [Pt(L6)(DMS)Cl] complex gives both the mono-solvolysis [(Pt(L6)(DMS)(CH_3CN)]$^+$ and the bi-solvolysis [(Pt(L6)(CH_3CN)$_2$]$^+$ species, which also reflected on the interaction with the 9-MeG where subsequently the monofunctional adduct [Pt(L6)(DMS)(9-MeG)]$^+$ as well as the bifunctional [Pt(L6)(9-MeG)$_2$]$^+$ and the N7,O6-bidentate 9-MeG [Pt(L6)(N7,O6-9-MeG)]$^+$ adducts were obtained. In summary, these findings indicate that such heteroleptic mono-chelate complexes can bind guanines similarly to Cisplatin and its analogues. First *in-vitro* studies using ovarian cancer cell lines revealed no superior activity compared to Cisplatin but point to a different mode-of-action because Cisplatin resistant cells respond similar or even better (lower IC_{50}) than Cisplatin sensitive cells to these compounds.

Experimental Section

Materials and techniques

All syntheses were carried out under nitrogen atmosphere. The ^{1}H, ^{13}C{1H}, ^{195}Pt NMR spectra were recorded with a Bruker Avance 400, 500 and 600 MHz spectrometer and the chemical shifts are given in ppm with $SiMe_4$ as internal references. Mass spectra were recorded with a Finnigan MAT SSQ 710 instrument. Elemental analysis was performed with a Leco CHNS-932 apparatus. TLC was performed by using Merck TLC aluminum sheets (Silica gel 60 F254). Solvents from Fisher Scientific and other chemicals from TCI, abcr and Sigma-Aldrich were used without further purification.

Synthesis of free ligands (HL1–HL9)

2′-Methylacetophenone (2.68 g, 2.62 ml, 20 mmol) for (HL1), 3′-methylacetophenone (2.68 g, 2.72 ml, 20 mmol) for (HL2), 4′-methylacetophenone (2.68 g, 2.67 ml, 20 mmol) for (HL3), 2′-methoxyacetophenone (3.00 g, 2.75 ml, 20 mmol) for (HL4), 3′-methoxyacetophenone (3.00 g, 2.75 ml, 20 mmol) for (HL5), 4′-methoxyacetophenone (3.00 g, 20 mmol) for (HL6), 2′-bromoacetophenone (3.98 g, 2.70 ml, 20 mmol) for (HL7), 3′-Bromoacetophenone (3.98 g, 2.65 ml, 20 mmol) for (HL8) and 4′-bromoacetophenone (3.98 g, 20 mmol) for (HL9), in dry diethyl ether (20 mL) were added slowly and separately to a precooled suspension of potassium tert-butoxide (4.49 g, 40 mmol) in dry diethyl ether (40 mL) at −78 °C. Carbon disulfide (1.7 ml, 28 mmol) was added dropwise to the solution under vigorous stirring, the mixture maintained at −78 °C for 3 hours and allowed to warm up to room temperature then a solution of 2-bromoacetic acid (2.28 g, 20 mmol) in dry diethyl ether (10 mL) was added dropwise with stirring to the formed dithiolate anion, the mixture is stirred protected from light at room temperature for a further 18 hours. For workup, the solvent was removed, and dichloromethane (100 ml) was added to the yellow crude product. Sulfuric acid (aqueous solution, 2 M, 100 ml) was added to the suspension and stirred for 30 minutes at room temperature. The two-phased system was separated, and the aqueous phase extracted with dichloromethane (3×35 ml). The combined organic phases were washed with water (3×20 ml), dried with sodium sulfate. After filtration, the solvent was removed, and the yellow crude product washed three times with n-pentane then recrystallized from (dichloromethane/acetone) affording the pure ligands HL1–HL9 with yields ranging from 7.21 % to 49.51 %. All compounds were characterized by NMR spectroscopy, mass spectrometry and elemental analyses (Ligand characterization data are described in detail in the supporting information).

General procedure for the Synthesis of platinum(II) complexes

A hot ethanolic solution of HL1–HL9 (1 equiv.) (20 mL) was added separately to a stirred suspension of cis-[$PtCl_2$(DMS)(DMSO)], (1 equiv.) in ethanol (20 mL). The resulting solution was stirred for 30 min. in hot water bath over 60 °C and then overnight at room temperature. The yellow solution turned red, and the solvent was removed under reduced pressure. The residue was purified by column chromatography using (cyclohexane/CH_2Cl_2/acetone, 5 : 2 : 1) as eluent affording three different classes of complexes, the first fraction is the bis-chelates [Pt(L1–L9)$_2$] while the second and third fractions are the mono-chelates [Pt(L1–L9)(DMS)Cl] and [Pt-(L1–L9)(DMSO)Cl], respectively. The products were obtained as a red or orange solids. (^{1}H, ^{13}C{^{1}H} and ^{195}Pt NMR spectra are shown in the supporting information Figures S7–S63)

HL1 (265 mg, 0.99 mmol), *cis*-[$PtCl_2$(DMS)(DMSO)] (400 mg, 0.99 mmol).

[Pt(L1)$_2$] ($PtC_{28}H_{30}O_6S_4$) (Mol. Wt.: 785.87 g/mol)

Red solid; yield: 70.30 mg (9.08 %); Rf = 0.8 (cyclohexane/CH_2Cl_2/acetone, 5 : 2 : 1).

^{1}H NMR (400 MHz, CD_2Cl_2) δ 7.48–7.39 (m, 2H), 7.39–7.30 (m, 2H), 7.19 (t, *J* = 7.0 Hz, 4H), 6.78 (s, 2H, =CH–), 4.24 (q, *J* = 7.1 Hz, 4H), 3.97 (s, 4H), 2.38 (s, 6H), 1.31 (t, *J* = 7.1 Hz, 6H), ^{13}C{^{1}H} NMR (101 MHz, CD_2Cl_2) δ 180.28 (–C=S), 173.97, 167.35, 139.95, 136.54, 131.26, 130.02, 126.98, 125.64, 116.71 (=CH–), 62.16, 36.44, 20.28, 13.93, ^{195}Pt NMR (85.7 MHz, CD_2Cl_2) δ −2296 ppm. ESI-MS: (positive mode *m/z*) 808.8 [M + Na]$^+$, elemental analysis for $PtC_{28}H_{30}O_6S_4$: C 42.79, H 3.85, S 16.32; found: C 42.57, H: 3.93 S: 16.29.

[Pt(L1)(DMS)Cl] ($PtC_{16}H_{21}O_3S_3Cl$) (Mol. Wt.: 588.06 g/mol)

Orange solid; yield: 162.2 mg (28 %); Rf = 0.6 (cyclohexane/CH_2Cl_2/acetone, 5 : 2 : 1).

^{1}H NMR (400 MHz, CD_2Cl_2) δ 7.42 (d, *J* = 7.7 Hz, 1H), 7.37 (td, *J* = 7.6, 1.2 Hz, 1H), 7.31–7.14 (m, 2H), 6.84 (s, 1H, =CH–), 4.23 (q, *J* = 7.1 Hz, 2H), 3.94 (s, 2H), 2.57 (s w/Pt satellites, $^3J_{Pt\text{-}H}$ = 51.04 Hz, 6H), 2.41 (s,

3H), 1.28 (t, $J=7.1$ Hz, 3H), $^{13}C\{^1H\}$ NMR (101 MHz, CD_2Cl_2) δ 179.48 (–C=S), 173.85, 167.31, 139.46, 137.19, 131.48, 130.32, 127.21, 125.66, 115.75 (=CH–), 62.20, 36.47, 23.88 (s w/Pt satellites, $^2J_{Pt\text{-}C}=18.78$ Hz, CH_3(DMS)), 20.74, 13.93, ^{195}Pt NMR (85.7 MHz, CD_2Cl_2) δ −2892 ppm, ESI-MS: (positive mode *m/z*) 611.1 $[M+Na]^+$, elemental analysis for $PtC_{16}H_{21}O_3S_3Cl$: C 32.68, H 3.60, S 16.36, Cl 6.03; found: C 32.65, H: 3.68 S: 16.47 Cl 5.96.

[Pt(L1)(DMSO)Cl] ($PtC_{16}H_{21}O_4S_3Cl$) (Mol. Wt.: 604.05 g/mol)

Orange solid; yield: 148 mg (24.87%); Rf = 0.5 (cyclohexane/CH_2Cl_2/acetone, 5:2:1).

^1H NMR (400 MHz, CD_2Cl_2) δ 7.42 (d, $J=7.7$ Hz, 1H), 7.37 (t, $J=7.5$ Hz, 1H), 7.21 (m, 2H), 6.81 (s, 1H, =CH–), 4.22 (q, $J=7.1$ Hz, 2H), 3.98 (s, 2H), 3.59 (s w/Pt satellites, $^3J_{Pt\text{-}H}=20.88$ Hz, 6H), 2.41 (s, 3H), 1.27 (t, $J=7.1$ Hz, 3H), $^{13}C\{^1H\}$ NMR (101 MHz, CD_2Cl_2) δ 180.47 (–C=S), 177.35, 167.21, 138.54, 137.51, 131.52, 130.62, 127.71, 125.71, 115.64 (=CH–), 62.31, 46.68(s w/Pt satellites, $^2J_{Pt\text{-}C}=50$ Hz, CH_3(DMSO)), 36.54, 20.81, 13.88, ^{195}Pt NMR (85.7 MHz, CD_2Cl_2) δ −3035 ppm, ESI-MS: (positive mode *m/z*) 626.9 $[M+Na]^+$, elemental analysis for $PtC_{16}H_{21}O_4S_3Cl$: C 31.81, H 3.50, S 15.92, Cl 5.87; found: C 32.05, H: 3.66 S: 15.83 Cl 5.89.

HL2 (265 mg, 0.99 mmol), *cis*-[$PtCl_2$(DMS)(DMSO)] (400 mg, 0.99 mmol).

[Pt(L2)$_2$] ($PtC_{28}H_{30}O_6S_4$) (Mol. Wt.: 785.87 g/mol)

Red solid; yield: 50.7 mg (6.55%); Rf = 0.7 (cyclohexane/CH_2Cl_2/acetone, 5:2:1).

^1H NMR (400 MHz, CD_2Cl_2) δ 7.83 (s, 2H), 7.75 (d, $J=7.8$ Hz, 2H), 7.35 (d, $J=7.6$ Hz, 2H), 7.27 (t, $J=7.7$ Hz, 2H), 7.23 (s, 2H, =CH–), 4.16 (q, $J=7.1$ Hz, 4H), 3.89 (s, 4H), 2.38 (s, 6H), 1.22 (t, $J=7.1$ Hz, 6H), $^{13}C\{^1H\}$ NMR (101 MHz, CD_2Cl_2) δ 175.19 (–C=S), 173.63, 167.48, 138.84, 138.21, 132.59, 128.71, 128.15, 124.39, 112.93 (=CH–), 62.14, 36.52, 21.23, 13.94, ^{195}Pt NMR (85.7 MHz, CD_2Cl_2) δ −2322 ppm, ESI-MS: (positive mode *m/z*) 808.8 $[M+Na]^+$, elemental analysis for $PtC_{28}H_{30}O_6S_4$: C 42.79, H 3.85, S 16.32; found: C 43.35, H: 3.87 S: 16.26.

[Pt(L2)(DMS)Cl] ($PtC_{16}H_{21}O_3S_3Cl$) (Mol. Wt.: 588.06 g/mol)

Orange solid; yield: 82 mg (14.15%); Rf = 0.5 (cyclohexane/CH_2Cl_2/acetone, 5:2:1).

^1H NMR (500 MHz, CD_2Cl_2) δ 7.74 (d, $J=7.3$ Hz, 2H), 7.40 (d, $J=7.4$ Hz, 1H), 7.32 (t, $J=8.0$ Hz, 1H), 7.23 (s, 1H, =CH–), 4.23 (q, $J=7.1$ Hz, 2H), 3.96 (s, 2H), 2.56 (s w/Pt satellites, $^3J_{Pt\text{-}H}=50.40$ Hz, 6H), 2.42 (s, 3H), 1.28 (t, $J=7.1$ Hz, 3H), $^{13}C\{^1H\}$ NMR (126 MHz, CD_2Cl_2) δ 175.49 (–C=S), 173.77, 167.78, 139.20, 138.29, 133.10, 129.11, 128.42, 125.16, 112.63 (=CH–), 62.55, 36.86, 24.24 (s w/Pt satellites, $^2J_{Pt\text{-}C}=18$ Hz, CH_3(DMS)), 21.49, 14.29, ^{195}Pt NMR (107 MHz, CD_2Cl_2) δ −2917 ppm, ESI-MS: (positive mode *m/z*) 611.1 $[M+Na]^+$, elemental analysis for $PtC_{16}H_{21}O_3S_3Cl$: C 32.68, H 3.60, S 16.36, Cl 6.03; found: C 32.87, H: 3.88 S: 16.21 Cl 5.81.

[Pt(L2)(DMSO)Cl] ($PtC_{16}H_{21}O_4S_3Cl$) (Mol. Wt.: 604.05 g/mol)

Orange solid; yield: 97.3 mg (13.13%); Rf = 0.4 (cyclohexane/CH_2Cl_2/acetone, 5:2:1).

^1H NMR (400 MHz, CD_2Cl_2) δ 7.75 (d, $J=5.9$ Hz, 2H), 7.41 (d, $J=7.5$ Hz, 1H), 7.33 (t, $J=8.0$ Hz, 1H), 7.20 (s, 1H, =CH–), 4.24 (q, $J=7.1$ Hz, 2H), 4.01 (s, 2H), 3.62 (s w/Pt satellites, $^3J_{Pt\text{-}H}=21.60$ Hz, 6H), 2.42 (s, 3H), 1.29 (t, $J=7.1$ Hz, 3H), $^{13}C\{^1H\}$ NMR (101 MHz, CD_2Cl_2) δ 176.81(–C=S), 176.15, 167.32, 138.87, 137.04, 133.15, 128.76, 128.39, 125.15, 112.12 (=CH–), 62.29, 46.76(s w/Pt satellites, $^2J_{Pt\text{-}C}=57.4$ Hz, CH_3(DMSO)), 36.58, 21.12, 13.87, ^{195}Pt NMR (85.7 MHz, CD_2Cl_2) δ −3058 ppm, ESI-MS: (positive mode *m/z*) 626.9 $[M+Na]^+$, elemental analysis for $PtC_{16}H_{21}O_4S_3Cl$: C 31.81, H 3.50, S 15.92, Cl 5.87; found: C 32.01, H: 3.73 S: 15.87 Cl 5.72.

HL3 (265 mg, 0.99 mmol), *cis*-[$PtCl_2$(DMS)(DMSO)] (400 mg, 0.99 mmol).

[Pt(L3)$_2$] ($PtC_{28}H_{30}O_6S_4$) (Mol. Wt.: 785.87 g/mol)

Red solid; yield: 50 mg (6.46%); Rf = 0.7 (cyclohexane/CH_2Cl_2/acetone, 5:2:1).

^1H NMR (400 MHz, CD_2Cl_2) δ 7.95 (d, $J=8.3$ Hz, 4H), 7.29 (d, $J=8.1$ Hz, 4H), 7.20 (s, 2H, =CH–), 4.24 (q, $J=7.1$ Hz, 4H), 3.97 (s, 4H), 2.38 (s, 6H), 1.31 (t, $J=7.1$ Hz, 6H), $^{13}C\{^1H\}$ NMR (101 MHz, CD_2Cl_2) δ 175.26 (–C=S), 172.98, 167.55, 142.79, 135.63, 129.65, 129.32, 127.69, 127.39, 112.82 (=CH–), 62.13, 36.49, 21.44, 13.93, ^{195}Pt NMR (85.7 MHz, CD_2Cl_2) δ −2330 ppm, ESI-MS: (positive mode *m/z*) 808.8 $[M+Na]^+$, elemental analysis for $PtC_{28}H_{30}O_6S_4$: C 42.79, H 3.85, S 16.32; found: C 42.63, H: 3.91 S: 16.22.

[Pt(L3)(DMS)Cl] ($PtC_{16}H_{21}O_3S_3Cl$) (Mol. Wt.: 588.06 g/mol)

Orange solid; yield: 102 mg (17.60%); Rf = 0.5 (cyclohexane/CH_2Cl_2/acetone, 5:2:1).

^1H NMR (400 MHz, CD_2Cl_2) δ 7.85 (d, $J=8.2$ Hz, 2H), 7.23 (s, 1H, =CH–), 7.23 (d, $J=8.0$ Hz, 2H), 4.22 (q, $J=7.1$ Hz, 2H), 3.94 (s, 2H), 2.55 (s w/Pt satellites, $^3J_{Pt\text{-}H}=49.60$ Hz, 6H), 2.34 (s, 3H), 1.27 (t, $J=7.1$ Hz, 3H), $^{13}C\{^1H\}$ NMR (101 MHz, CD_2Cl_2) δ 174.90 (–C=S), 172.85, 167.48, 143.09, 135.09, 129.65, 127.69, 111.93 (=CH–), 62.18, 36.50, 23.89 (s w/Pt satellites, $^2J_{Pt\text{-}C}=19.79$ Hz, CH_3(DMS)), 21.43, 13.93, ^{195}Pt NMR (85.7 MHz, CD_2Cl_2) δ −2923 ppm, ESI-MS: (positive mode *m/z*) 611.1 $[M+Na]^+$, elemental analysis for $PtC_{16}H_{21}O_3S_3Cl$: C 32.68, H 3.60, S 16.36, Cl 6.03; found: C 32.75, H: 3.83 S: 16.44 Cl 6.11.

[Pt(L3)(DMSO)Cl] ($PtC_{16}H_{21}O_4S_3Cl$) (Mol. Wt.: 604.05 g/mol)

Orange solid; yield: 45 mg (7.56%); Rf = 0.3 (cyclohexane/CH_2Cl_2/acetone, 5:2:1).

^1H NMR (600 MHz, CD_2Cl_2) δ 7.87 (d, $J=8.3$ Hz, 2H), 7.26 (d, $J=8.0$ Hz, 2H), 7.22 (s, 1H, =CH–), 4.23 (q, $J=7.1$ Hz, 2H), 4.00 (s, 2H), 3.61 (s w/Pt satellites, $^3J_{Pt\text{-}H}=17.60$ Hz, 6H), 2.37 (s, 3H), 1.29 (t, $J=7.1$ Hz, 3H), $^{13}C\{^1H\}$ NMR (151 MHz, CD_2Cl_2) δ 176.31 (–C=S), 175.96, 167.56, 143.80, 134.33, 129.82, 128.18, 111.90 (=CH–), 62.45, 46.90 (s w/Pt satellites, $^2J_{Pt\text{-}C}=49.5$ Hz, CH_3(DMSO)), 36.71, 21.59, 14.03. ^{195}Pt NMR (85.7 MHz, CD_2Cl_2) δ −3067 ppm, ESI-MS: (positive mode *m/z*) 626.9 $[M+Na]^+$, elemental analysis for $PtC_{16}H_{21}O_4S_3Cl$: C 31.81, H 3.50, S 15.92, Cl 5.87; found: C 32.13, H: 3.69 S: 16.04 Cl 5.76.

HL4 (280 mg, 0.99 mmol), cis-[PtCl2(DMS)(DMSO)] (400 mg, 0.99 mmol).

[Pt(L4)2] (PtC28H30O8S4) (Mol. Wt.: 817.86 g/mol)

Red solid; yield: 37.5 mg (4.65%); Rf = 0.8 (cyclohexane/CH2Cl2/acetone, 5:2:1).

^1H NMR (400 MHz, CD_2Cl_2) δ 7.74 (dd, $J=7.7$, 1.6 Hz, 2H), 7.56–7.42 (m, 2H), 7.23 (s, 2H, =CH–), 7.08–6.89 (m, 4H), 4.24 (q, $J=7.1$ Hz, 4H), 3.96 (s, 4H), 3.89 (s, 6H), 1.30 (t, $J=7.1$ Hz, 6H), $^{13}C\{^1H\}$ NMR (101 MHz, CD_2Cl_2) δ 175.69 (–C=S), 171.90, 167.52, 156.99, 132.33, 130.31, 128.75, 120.82, 117.68, 112.11 (=CH–), 62.09, 55.85, 36.47, 13.92, ^{195}Pt NMR (85.7 MHz, CD_2Cl_2) δ −2300 ppm, ESI-MS: (positive mode *m/z*) 840 $[M+Na]^+$, elemental analysis for $PtC_{28}H_{30}O_8S_4$: C 41.12, H 3.70, S 15.68; found: C 40.99, H: 3.68 S: 15.71.

[Pt(L4)(DMS)Cl] ($PtC_{16}H_{21}O_4S_3Cl$) (Mol. Wt.: 604.05 g/mol)

Orange solid; yield: 60 mg (10.10%); Rf = 0.7 (cyclohexane/CH_2Cl_2/acetone, 5:2:1).

^{1}H NMR (400 MHz, CD_2Cl_2) δ 7.71 (dd, J = 7.8, 1.6 Hz, 1H), 7.58–7.42 (m, 1H), 7.32 (s, 1H, =CH–), 7.10–6.89 (m, 2H), 4.22 (q, J = 7.1 Hz, 2H), 3.94 (s, 2H), 3.89 (s, 3H), 2.56 (s w/Pt satellites, $^{3}J_{Pt\text{-}H}$ = 49.20 Hz, 6H), 1.27 (t, J = 7.0 Hz, 3H), ^{13}C{^{1}H} NMR (101 MHz, CD_2Cl_2) δ 174.91 (–C=S), 171.80, 167.43, 156.96, 132.59, 130.88, 128.18, 120.99, 116.84, 112.07 (=CH–), 62.13, 55.87, 36.51, 23.86 (s w/Pt satellites, $^{2}J_{Pt\text{-}C}$ = 19.79 Hz, CH_3(DMS)), 13.92, ^{195}Pt NMR (85.7 MHz, CD_2Cl_2) δ −2905 ppm, ESI-MS: (positive mode *m/z*) 626.9 $[M+Na]^+$, elemental analysis for $PtC_{16}H_{21}O_4S_3Cl$: C 31.81, H 3.50, S 15.92, Cl 5.87; found: C 31.75, H: 3.64 S: 16.07 Cl 5.59.

[Pt(L4)(DMSO)Cl] ($PtC_{16}H_{21}O_5S_3Cl$) (Mol. Wt.: 620.05 g/mol)

Orange solid; yield: 45 mg (7.37%); Rf = 0.4 (cyclohexane/CH_2Cl_2/acetone, 5:2:1).

^{1}H NMR (400 MHz, CD_2Cl_2) δ 7.75 (dd, J = 7.8, 1.7 Hz, 1H), 7.56–7.42 (m, 1H), 7.35 (s, 1H, =CH–), 7.11–6.92 (m, 2H), 4.22 (q, J = 7.1 Hz, 2H), 3.99 (s, 2H), 3.90 (s, 3H), 3.61 (s w/Pt satellites, $^{3}J_{Pt\text{-}H}$ = 20.80 Hz, 6H), 1.28 (t, J = 7.1 Hz, 3H), ^{13}C{^{1}H} NMR (101 MHz, CD_2Cl_2) δ 175.60 (–C=S), 175.33, 167.32, 157.40, 133.04, 131.24, 127.14, 120.99, 116.65, 112.05 (=CH–), 62.23, 55.88, 46.71 (s w/Pt satellites, $^{2}J_{Pt\text{-}C}$ = 59.67 Hz, CH_3(DMSO), 36.57, 13.86, ^{195}Pt NMR (85.7 MHz, CD_2Cl_2) δ −3048 ppm, ESI-MS: (positive mode *m/z*) 642.9 $[M+Na]^+$, elemental analysis for $PtC_{16}H_{21}O_5S_3Cl$: C 30.99, H 3.41, S 15.51, Cl 5.72; found: C 30.87, H: 3.56 S: 15.48 Cl 5.66.

HL5 (182 mg, 0.64 mmol), *cis*-[$PtCl_2$(DMS)(DMSO)] (260 mg, 0.64 mmol).

[Pt(L5)$_2$] ($PtC_{28}H_{30}O_8S_4$) (Mol. Wt.: 817.86 g/mol)

Red solid; yield: 31.70 mg (6.05%); Rf = 0.8 (cyclohexane/CH_2Cl_2/acetone, 5:2:1).

^{1}H NMR (600 MHz, CD_2Cl_2) δ 7.63 (s, 2H), 7.59 (d, J = 7.9 Hz, 2H), 7.34 (t, J = 8.0 Hz, 2H), 7.21 (s, 2H, =CH–), 7.14 (ddd, J = 8.2, 2.6, 0.7 Hz, 2H), 4.25 (q, J = 7.1 Hz, 4H), 3.97 (s, 4H), 3.88 (s, 6H), 1.31 (t, J = 7.1 Hz, 6H), ^{13}C{^{1}H} NMR (151 MHz, CD_2Cl_2) δ 174.87 (–C=S), 174.18, 167.63, 160.35, 139.93, 129.90, 119.56, 117.96, 113.13, 112.60 (=CH–), 62.34, 55.55, 36.71, 14.08, ^{195}Pt NMR (85.7 MHz, CD_2Cl_2) δ −2316 ppm, ESI-MS: (positive mode *m/z*) 840 $[M+Na]^+$, elemental analysis for $PtC_{28}H_{30}O_8S_4$: C 41.12, H 3.70, S 15.68; found: C 41.27, H: 3.90 S: 15.59.

[Pt(L5)(DMS)Cl] ($PtC_{16}H_{21}O_4S_3Cl$) (Mol. Wt.: 604.05 g/mol)

Orange solid; yield: 54.40 mg (14.09%); Rf = 0.7 (cyclohexane/CH_2Cl_2/acetone, 5:2:1).

^{1}H NMR (400 MHz, CD_2Cl_2) δ 7.52 (d, J = 7.8 Hz, 1H), 7.48 (s, 1H), 7.34 (t, J = 8.0 Hz, 1H), 7.22 (s, 1H, =CH–), 7.12 (dd, J = 8.0, 2.2 Hz, 1H), 4.23 (q, J = 7.1 Hz, 2H), 3.95 (s, 2H), 3.85 (s, 3H), 2.56 ((s w/Pt satellites, $^{3}J_{Pt\text{-}H}$ = 50 Hz, 6H), 1.28 (t, J = 7.1 Hz, 3H), ^{13}C{^{1}H} NMR (101 MHz, CD_2Cl_2) δ 174.52 (–C=S), 173.91, 167.42, 160.09, 139.37, 129.86, 119.84, 117.79, 112.74, 112.22 (=CH–), 62.22, 55.42, 36.57, 23.92 (s w/Pt satellites, $^{2}J_{Pt\text{-}C}$ = 23.83 Hz, CH_3(DMS)), 13.93, ^{195}Pt NMR (85.7 MHz, CD_2Cl_2) δ −2912 ppm, ESI-MS: (positive mode *m/z*) 626.9 $[M+Na]^+$, elemental analysis for $PtC_{16}H_{21}O_4S_3Cl$: C 31.81, H 3.50, S 15.92, Cl 5.87; found: C 31.65, H: 3.58 S: 16.03 Cl 5.76.

[Pt(L5)(DMSO)Cl] ($PtC_{16}H_{21}O_5S_3Cl$) (Mol. Wt.: 620.05 g/mol)

Orange solid; yield: 67.10 mg (16.90%); Rf = 0.5 (cyclohexane/CH_2Cl_2/acetone, 5:2:1).

^{1}H NMR (400 MHz, CD_2Cl_2) δ 7.52 (d, J = 7.9 Hz, 1H), 7.48 (s, 1H), 7.35 (t, J = 8.0 Hz, 1H), 7.18 (s, 1H, =CH–), 7.12 (dd, J = 8.2, 2.4 Hz, 1H), 4.23 (q, J = 7.1 Hz, 2H), 4.01 (s, 2H), 3.85 (s, 3H), 3.62 (s w/Pt satellites, $^{3}J_{Pt\text{-}H}$ = 18.50 Hz, 6H), 1.29 (t, J = 7.2 Hz, 3H), ^{13}C{^{1}H} NMR (101 MHz, CD_2Cl_2) δ 177.31 (–C=S), 175.42, 167.32, 160.05, 138.42, 129.85, 120.17, 118.18, 113.04, 112.02 (=CH–), 62.31, 55.42, 46.76 (s w/Pt satellites, $^{2}J_{Pt\text{-}C}$ = 58.7 Hz, CH_3(DMSO)), 36.65, 13.87, ^{195}Pt NMR (85.7 MHz, CD_2Cl_2) δ −3053 ppm, ESI-MS: (positive mode *m/z*) 642.9 $[M+Na]^+$, elemental analysis for $PtC_{16}H_{21}O_5S_3Cl$: C 30.99, H 3.41, S 15.51, Cl 5.72; found: C 31.02, H: 3.45 S: 15.43 Cl 5.80.

HL6 (140 mg, 0.49 mmol), *cis*-[$PtCl_2$(DMS)(DMSO)] (200 mg, 0.49 mmol).

[Pt(L6)$_2$] ($PtC_{28}H_{30}O_8S_4$) (Mol. Wt.: 817.86 g/mol)

Red solid; yield: 32 mg (7.94%); Rf = 0.8 (cyclohexane/CH_2Cl_2/acetone, 5:2:1).

^{1}H NMR (400 MHz, CD_2Cl_2) δ 8.04 (d, J = 8.9 Hz, 4H), 7.19 (s, 2H, =CH–), 6.98 (d, J = 8.9 Hz, 4H), 4.24 (q, J = 7.1 Hz, 4H), 3.96 (s, 4H), 3.88 (s, 6H), 1.31 (t, J = 7.1 Hz, 6H), ^{13}C{^{1}H} NMR (101 MHz, CD_2Cl_2) δ 174.66 (–C=S), 171.88, 167.67, 162.79, 130.72, 129.50, 114.22, 112.53 (=CH–), 62.11, 55.54, 36.46, 13.94, ^{195}Pt NMR (85.7 MHz, CD_2Cl_2) δ −2350 ppm, ESI-MS: (positive mode *m/z*) 840 $[M+Na]^+$, elemental analysis for $PtC_{28}H_{30}O_8S_4$: C 41.12, H 3.70, S 15.68; found: C 40.69, H: 3.65 S: 15.78.

[Pt(L6)(DMS)Cl] ($PtC_{16}H_{21}O_4S_3Cl$) (Mol. Wt.: 604.05 g/mol)

Orange solid; yield: 33 mg (11.07%); Rf = 0.7 (cyclohexane/CH_2Cl_2/acetone, 5:2:1).

^{1}H NMR (500 MHz, CD_2Cl_2) δ 7.95 (d, J = 9.0 Hz, 2H), 7.22 (s, 1H, =CH–), 6.93 (d, J = 9.0 Hz, 2H), 4.22 (q, J = 7.1 Hz, 2H), 3.94 (s, 2H), 3.85 (s, 3H), 2.55 ((s w/Pt satellites, $^{3}J_{Pt\text{-}H}$ = 46.50 Hz, 6H), 1.28 (t, J = 7.1 Hz, 3H), ^{13}C{^{1}H} NMR (126 MHz, CD_2Cl_2) δ 174.31 (–C=S), 171.72, 167.62, 163.01, 130.11, 129.91, 114.22, 111.57 (=CH–), 62.18, 55.55, 36.48, 23.87(s w/Pt satellites, $^{2}J_{Pt\text{-}C}$ = 19.50 Hz, CH_3(DMS)), 13.96, ^{195}Pt NMR (107 MHz, CD_2Cl_2) δ −2937 ppm, ESI-MS: (positive mode *m/z*) 626.9 $[M+Na]^+$, elemental analysis for $PtC_{16}H_{21}O_4S_3Cl$: C 31.81, H 3.50, S 15.92, Cl 5.87; found: C 32.05, H: 3.53 S: 16.13 Cl 5.93.

[Pt(L6)(DMSO)Cl] ($PtC_{16}H_{21}O_5S_3Cl$) (Mol. Wt.: 620.05 g/mol)

Orange solid; yield: 7 mg (2.29%); Rf = 0.4 (cyclohexane/CH_2Cl_2/acetone, 5:2:1).

^{1}H NMR (500 MHz, CD_2Cl_2) δ 7.97 (d, J = 9.0 Hz, 2H), 7.21 (s, 1H, =CH–), 6.94 (d, J = 9.0 Hz, 2H), 4.23 (q, J = 7.1 Hz, 2H), 3.99 (s, 2H), 3.86 (s, 3H), 3.61 (s w/Pt satellites, $^{3}J_{Pt\text{-}H}$ = 18.68 Hz, 6H), 1.29 (t, J = 7.1 Hz, 3H), ^{13}C{^{1}H} NMR (126 MHz, CD_2Cl_2) δ 175.30 (–C=S), 174.88, 167.52, 163.39, 130.29, 129.20, 114.24, 111.43 (=CH–), 62.27, 55.58, 46.75(s w/Pt satellites, $^{2}J_{Pt\text{-}C}$ = 59.87 Hz, CH_3(DMSO)), 36.52, 13.89, ^{195}Pt NMR 107 MHz, CD_2Cl_2) δ −3079 ppm, ESI-MS: (positive mode *m/z*) 642.9 $[M+Na]^+$, elemental analysis for $PtC_{16}H_{21}O_5S_3Cl$: C 30.99, H 3.41, S 15.51, Cl 5.72; found: C 31.04, H: 3.52 S: 15.63 Cl 5.59.

HL7 (300 mg, 0.91 mmol), *cis*-[$PtCl_2$(DMS)(DMSO)] (370 mg, 0.91 mmol).

[Pt(L7)$_2$] ($PtC_{26}H_{24}O_6S_4Br_2$) (Mol. Wt.: 915.60 g/mol)

Red solid; yield: 50 mg (5.99%); Rf = 0.8 (cyclohexane/CH_2Cl_2/acetone, 5:2:1).

^{1}H NMR (400 MHz, $CDCl_3$) δ 7.55 (dd, J = 7.8, 1.2 Hz, 2H), 7.51 (dd, J = 7.5, 1.9 Hz, 2H), 7.32–7.22 (m, 4H), 6.76 (s, 2H, =CH–), 4.27 (q, J = 7.1 Hz, 4H), 3.98 (s, 4H), 1.33 (t, J = 7.1 Hz, 6H), ^{13}C{^{1}H} NMR (101 MHz, $CDCl_3$) δ 177.01(–C=S), 175.06, 167.29, 141.25, 133.76, 131.06, 129.46, 127.23, 119.87, 116.89 (=CH–), 62.27, 36.52, 14.15, ^{195}Pt NMR (85.7 MHz, $CDCl_3$) δ −2267 ppm, ESI-MS: (positive mode *m/z*) 938.8 $[M+Na]^+$, elemental analysis for $PtC_{26}H_{24}O_6S_4Br_2$: C 34.11, H 2.64, S 14.01, Br 17.45; found: C 34.23, H: 2.88 S: 14.07, Br 17.36.

[Pt(L7)(DMS)Cl] ($PtC_{15}H_{18}O_3S_3BrCl$) (Mol. Wt.: 652.92 g/mol)

Orange solid; yield: 139.40 mg (23.43 %); Rf = 0.6 (cyclohexane/CH_2Cl_2/acetone, 5 : 2 : 1).

^{1}H NMR (400 MHz, $CDCl_3$) δ 7.56 (dd, J = 7.6, 1.4 Hz, 1H), 7.51 (dd, J = 7.4, 2.0 Hz, 1H), 7.36–7.20 (m, 2H), 6.85 (s, 1H, =CH–), 4.26 (q, J = 7.1 Hz, 2H), 3.95 (s, 2H), 2.61 (s w/Pt satellites, $^3J_{Pt\text{-}H}$ = 48.80 Hz, 6H), 1.30 (t, J = 7.1 Hz, 3H), $^{13}C\{^1H\}$ NMR (101 MHz, $CDCl_3$) δ 176.51 (–C=S), 174.42, 167.24, 140.99, 133.72, 131.21, 129.88, 127.39, 119.59, 116.48 (=CH–), 62.30, 36.50, 24.14(s w/Pt satellites, $^2J_{Pt\text{-}C}$ = 15.65 Hz, CH_3(DMS)), 14.13, ^{195}Pt NMR (85.7 MHz, $CDCl_3$) δ −2879 ppm, ESI-MS: (positive mode *m/z*) 675.8 $[M+Na]^+$, elemental analysis for $PtC_{15}H_{18}O_3S_3BrCl$: C 27.59, H 2.78, S 14.73, Br 12.24, Cl 5.43; found: C 27.75, H: 2.94 S: 14.57, Br 12.18, Cl 5.52.

[Pt(L7)(DMSO)Cl] ($PtC_{15}H_{18}O_4S_3BrCl$) (Mol. Wt.: 668.92 g/mol)

Orange solid; yield: 96.6 mg (15.85 %); Rf = 0.5 (cyclohexane/CH_2Cl_2/acetone, 5 : 2 : 1).

^{1}H NMR (400 MHz, $CDCl_3$) δ 7.58 (dd, J = 7.7, 1.2 Hz, 1H), 7.50 (dd, J = 7.5, 1.9 Hz, 1H), 7.38–7.25 (m, 2H), 6.82 (s, 1H, =CH–), 4.26 (q, J = 7.1 Hz, 2H), 4.04 (s, 2H), 3.65 (s w/Pt satellites, $^3J_{Pt\text{-}H}$ = 18.80 Hz, 6H), 1.31 (t, J = 7.1 Hz, 3H), $^{13}C\{^1H\}$ NMR (101 MHz, $CDCl_3$) δ 178.37 (–C=S), 177.20, 167.10, 140.10, 133.82, 131.45, 130.05, 127.42, 119.99, 116.18 (=CH–), 62.42, 46.80 (s w/Pt satellites, $^2J_{Pt\text{-}C}$ = 58.07 Hz, CH_3(DMSO), 36.67, 14.09, ^{195}Pt NMR (85.7 MHz, $CDCl_3$) δ −3033 ppm, ESI-MS: (positive mode *m/z*) 691.8 $[M+Na]^+$, elemental analysis for $PtC_{15}H_{18}O_4S_3BrCl$: C 26.93, H 2.71, S 14.38, Br 11.95, Cl 5.30; found: C 26.87, H: 2.56 S: 14.47, Br 12.03, Cl 5.32.

HL8 (300 mg, 0.91 mmol), *cis*-[$PtCl_2$(DMS)(DMSO)] (370 mg, 0.91 mmol).

[Pt(L8)$_2$] ($PtC_{26}H_{24}O_6S_4Br_2$) (Mol. Wt.: 915.60 g/mol)

Red solid; yield: 64.8 mg (7.77 %); Rf = 0.8 (cyclohexane/CH_2Cl_2/acetone, 5 : 2 : 1).

^{1}H NMR (400 MHz, $CDCl_3$) δ 8.15 (s, 2H), 7.91 (d, J = 7.9 Hz, 2H), 7.67 (d, J = 7.9 Hz, 2H), 7.30 (t, J = 7.9 Hz, 2H), 7.07 (s, 2H, =CH–), 4.27 (q, J = 7.1 Hz, 4H), 3.96 (s, 4H), 1.33 (t, J = 7.1 Hz, 6H), $^{13}C\{^1H\}$ NMR (101 MHz, $CDCl_3$) δ 175.32 (–C=S), 172.47, 167.37, 140.14, 134.38, 130.53, 130.37, 125.67, 123.25, 112.54 (=CH–), 62.27, 36.63, 14.17, ^{195}Pt NMR (85.7 MHz, $CDCl_3$) δ −2270 ppm, ESI-MS: (positive mode *m/z*) 938.8 $[M+Na]^+$, elemental analysis for $PtC_{26}H_{24}O_6S_4Br_2$: C 34.11, H 2.64, S 14.01, Br 17.45; found: C 34.28, H: 2.86 S: 13.87, Br 17.33.

[Pt(L8)(DMS)Cl] ($PtC_{15}H_{18}O_3S_3BrCl$) (Mol. Wt.: 652.92 g/mol)

Orange solid; yield: 100 mg (16.81 %); Rf = 0.6 (cyclohexane/CH_2Cl_2/acetone, 5 : 2 : 1).

^{1}H NMR (400 MHz, $CDCl_3$) δ 8.06 (s, 1H), 7.92 (d, J = 8.0 Hz, 1H), 7.68 (d, J = 8.0 Hz, 1H), 7.33–7.26 (m, 1H), 7.15 (s, 1H, =CH–), 4.27 (q, J = 7.1 Hz, 2H), 3.96 (s, 2H), 2.62 (s w/Pt satellites, $^3J_{Pt\text{-}H}$ = 47.20 Hz, 6H), 1.31 (t, J = 7.1 Hz, 3H), $^{13}C\{^1H\}$ NMR (101 MHz, $CDCl_3$) δ 174.92(–C=S), 173.08, 167.32, 139.92, 134.64, 130.44, 130.37, 126.50, 122.97, 112.19 (=CH–), 62.33, 36.53, 24.17(s w/Pt satellites, $^2J_{Pt\text{-}C}$ = 18.50 Hz, CH_3(DMS)), 14.16, ^{195}Pt NMR (85.7 MHz, $CDCl_3$) δ −2902 ppm, ESI-MS: (positive mode *m/z*) 675.8 $[M+Na]^+$, elemental analysis for $PtC_{15}H_{18}O_3S_3BrCl$: C 27.59, H 2.78, S 14.73, Br 12.24, Cl 5.43; found: C 27.88, H: 2.96 S: 14.54, Br 12.11, Cl 5.64.

[Pt(L8)(DMSO)Cl] ($PtC_{15}H_{18}O_4S_3BrCl$) (Mol. Wt.: 668.92 g/mol)

Orange solid; yield: 65 mg (10.66 %); Rf = 0.5 (cyclohexane/CH_2Cl_2/acetone, 5 : 2 : 1).

^{1}H NMR (400 MHz, $CDCl_3$) δ 8.05 (s, 1H), 7.89 (d, J = 7.9 Hz, 1H), 7.66 (d, J = 8.0 Hz, 1H), 7.29 (t, J = 7.9 Hz, 1H), 7.09 (s, 1H, =CH–), 4.26 (q, J = 7.1 Hz, 2H), 4.04 (s, 2H), 3.65 (s w/Pt satellites, $^3J_{Pt\text{-}H}$ = 18.40 Hz, 6H), 1.31 (t, J = 7.1 Hz, 3H), $^{13}C\{^1H\}$ NMR (101 MHz, $CDCl_3$) δ 178.58 (–C=S), 173.75, 167.19, 138.99, 135.02, 130.71, 130.41, 126.66, 123.00, 111.92 (=CH–), 62.44, 46.87(s w/Pt satellites, $^2J_{Pt\text{-}C}$ = 56.86 Hz, CH_3(DMSO)), 36.70, 14.10, ^{195}Pt NMR (85.7 MHz, $CDCl_3$) δ −3054 ppm, ESI-MS: (positive mode *m/z*) 691.8 $[M+Na]^+$, elemental analysis for $PtC_{15}H_{18}O_4S_3BrCl$: C 26.93, H 2.71, S 14.38, Br 11.95, Cl 5.30; found: C 27.12, H: 2.99 S: 14.27, Br 11.83, Cl 5.44.

HL9 (330 mg, 0.99 mmol), *cis*-[$PtCl_2$(DMS)(DMSO)] (400 mg, 0.99 mmol).

[Pt(L9)$_2$] ($PtC_{26}H_{24}O_6S_4Br_2$) (Mol. Wt.: 915.60 g/mol)

Red solid; yield: 51 mg (5.65 %); Rf = 0.8 (cyclohexane/CH_2Cl_2/acetone, 5 : 2 : 1).

^{1}H NMR (400 MHz, $CDCl_3$) δ 7.86 (d, J = 8.6 Hz, 4H), 7.59 (d, J = 8.5 Hz, 4H), 7.11 (s, 2H, =CH–), 4.27 (q, J = 7.1 Hz, 4H), 3.98 (s, 4H), 1.33 (t, J = 7.1 Hz, 6H), $^{13}C\{^1H\}$ NMR (101 MHz, $CDCl_3$) δ 174.02 (–C=S), 171.28, 167.29, 137.57, 132.15, 128.71, 126.47, 112.86 (=CH–), 62.14, 36.55, 14.06, ^{195}Pt NMR (85.7 MHz, $CDCl_3$) δ −2303 ppm, ESI-MS: (positive mode *m/z*) 938.8 $[M+Na]^+$, elemental analysis for $PtC_{26}H_{24}O_6S_4Br_2$: C 34.11, H 2.64, S 14.01, Br 17.45; found: C 34.33, H: 2.82 S: 13.87, Br 17.61.

[Pt(L9)(DMS)Cl] ($PtC_{15}H_{18}O_3S_3BrCl$) (Mol. Wt.: 652.92 g/mol)

Orange solid; yield: 113 mg (17.57 %); Rf = 0.6 (cyclohexane/CH_2Cl_2/acetone, 5 : 2 : 1).

^{1}H NMR (500 MHz, $CDCl_3$) δ 7.84 (d, J = 8.7 Hz, 2H), 7.52 (d, J = 8.7 Hz, 2H), 7.16 (s, 1H, =CH–), 4.24 (q, J = 7.1 Hz, 2H), 3.93 (s, 2H), 2.60 (s w/Pt satellites, $^3J_{Pt\text{-}H}$ = 44.60 Hz, 6H), 1.29 (t, J = 7.1 Hz, 3H), $^{13}C\{^1H\}$ NMR (126 MHz, $CDCl_3$) δ 174.27 (–C=S), 173.46, 167.41, 136.67, 132.14, 129.29, 126.89, 111.92 (=CH–), 62.33, 36.51, 24.26 (s w/Pt satellites, $^2J_{Pt\text{-}C}$ = 18.25 Hz, CH_3(DMS)), 14.17, ^{195}Pt NMR (107 MHz, $CDCl_3$) δ −2907 ppm, ESI-MS: (positive mode *m/z*) 675.8 $[M+Na]^+$, elemental analysis for $PtC_{15}H_{18}O_3S_3BrCl$. 0.25 cyclohexane: C 29.40, H 3.14, S 14.27, Br 11.85, Cl 5.26; found: C 29.12, H: 2.93 S: 14.24, Br 11.70, Cl 5.48.

[Pt(L9)(DMSO)Cl] ($PtC_{15}H_{18}O_4S_3BrCl$) (Mol. Wt.: 668.92 g/mol)

Orange solid; yield: 87 mg (13.20 %); Rf = 0.5 (cyclohexane/CH_2Cl_2/acetone, 5 : 2 : 1).

^{1}H NMR (500 MHz, $CDCl_3$) δ 7.82 (d, J = 8.7 Hz, 2H), 7.54 (d, J = 8.7 Hz, 2H), 7.11 (s, 1H, =CH–), 4.26 (q, J = 7.2 Hz, 2H), 4.03 (s, 2H), 3.65 (s w/Pt satellites, $^3J_{Pt\text{-}H}$ = 17.95 Hz, 6H), 1.30 (t, J = 7.1 Hz, 3H), $^{13}C\{^1H\}$ NMR (126 MHz, $CDCl_3$) δ 177.87 (–C=S), 174.17, 167.29, 135.75, 132.17, 129.52, 127.34, 111.67 (=CH–), 62.43, 46.86 (s w/Pt satellites, $^2J_{Pt\text{-}C}$ = 55.87 Hz, CH_3(DMSO)), 36.68, 14.12, ^{195}Pt NMR (107 MHz, $CDCl_3$) δ −3060 ppm, ESI-MS: (positive mode *m/z*) 691.8 $[M+Na]^+$, elemental analysis for $PtC_{15}H_{18}O_4S_3BrCl$: C 26.93, H 2.71, S 14.38, Br 11.95, Cl 5.30; found: C 27.00, H: 2.83 S: 14.41, Br 12.05, Cl 5.28.

Stability and solvolysis of the Pt(II) complexes

As a typical experiment, 0.21–0.29 mg of [Pt(L6)$_2$], [Pt(L6)(DMS)Cl], and [Pt(L6)(DMSO)Cl] complexes were dissolved in 1 mL of CH_3CN: PBS buffer (pH 7.4; 1 : 1), to obtain a 0.35 mM solution, which was incubated at 37 °C for 72 hours. The ESI-MS spectra were recorded after 24, 48 and 72 hours.

Interactions of the Pt(II) complexes with 9-methylguanine

As a typical experiment, 0.21–0.29 mg of [Pt(L6)$_2$], [Pt(L6)(DMS)Cl], and [Pt(L6)(DMSO)Cl] complexes were dissolved in 1 mL of CH_3CN:

PBS buffer (pH 7.4; 1:1), to obtain a 0.35 mM solution, then (8 eq. 0.47 mg) of 9-MG was added and the mixtures were incubated at 37 °C for 72 hours. The ESI-MS spectra were recorded after 24, 48 and 72 hours.

IC_{50} determination

Cancer cell lines were cultured under standard conditions (5% CO_2, 37 °C, 90% humidity) in RPMI medium supplemented with 10% FCS, 100 U/ml penicillin and 100 μg/ml streptomycin (Life Technologies, Germany). The tested Pt(II) complexes was dissolved in DMSO. Determinations of IC_{50} values were carried out using the CellTiter96 non-radioactive proliferation assay (MTT assay, Promega). After seeding 5000 cells per well in a 96 well plate cells were allowed to attach for 24 h and were incubated for 48 h with different concentrations of the substances ranging from 0 to 100 μM for Metal complexes (0, 1, 3, 10, 33, 100 μM). Each measurement was done in triplicate and repeated 3-times. The proportion of live cells was quantified by the MTT assay and after background subtraction relative values compared to the mean of medium controls were calculated. Non-linear regression analyses applying the Hill-slope were run in GraphPad 5.0 software.

Acknowledgements

M.K.F. is grateful to the Katholischer Akademischer Ausländer-Dienst (KAAD) for a Ph.D. scholarship. The authors would further like to thank Umicore AG & Co. KG Hanau-Wolfgang, Germany for the donation of K_2PtCl_4. Open Access funding enabled and organized by Projekt DEAL.

Conflict of Interest

The authors declare no conflict of interest.

Data Availability Statement

The data that support the findings of this study are available from the corresponding author upon reasonable request.

Keywords: Platinum(II) complexes · β-hydroxydithiocinnamic esters ligands · O,S-bidentate chelating ligands · Stability and solvolysis · 9-methylguanine binding

[1] M. S. Singh, G. C. Nandi, T. Chanda, *RSC Adv.* **2013**, *3*, 14183–14198.
[2] J. Li, W. Ma, W. Ming, C. Xu, N. Wei, M. Wang, *J. Org. Chem.* **2015**, *80*, 11138–11142.
[3] S. Soni, S. Koley, M. S. Singh, *Tetrahedron Lett.* **2017**, *58*, 2512–2516.
[4] R. K. Chellu, S. Kurva, A. K. Soda, S. K. Chilaka, J. B. Nanubolu, S. Madabhushi, *Asian J. Org. Chem.* **2021**, *10*, 1432–1435.
[5] I. H. Chanu, L. M. Devi, T. P. Singh, S. J. Singh, R. R. Singh, O. Mukherjee Singh, *ChemistrySelect* **2020**, *5*, 7447–7451.
[6] D. Yadav, A. Srivastava, M. A. Ansari, M. S. Singh, *J. Org. Chem.* **2021**, *86*, 5908–5921.
[7] S. T. Bhaskaran, P. Mathew, *J. Mol. Struct.* **2022**, *1251*, 132071.
[8] K. Kumari, S. Kumar, K. N. Singh, M. G. B. Drew, N. Singh, *New J. Chem.* **2020**, *44*, 12143–12153.
[9] C. L. Yadav, G. R.. Anamika, G. Rajput, K. Kumar, M. G. B. Drew, N. Singh, *Inorg. Chem.* **2020**, *59*, 11417–11431.
[10] K. Kumari, A. S. Singh, K. K. Manar, C. L. Yadav, V. K. Tiwari, M. G. B. Drew, N. Singh, *New J. Chem.* **2019**, *43*, 1166–1176.
[11] M. K. Yadav, G. Rajput, K. Srivastava, R. K. Singh, R. Mishra, M. G. B. Drew, N. Singh, *New J. Chem.* **2015**, *39*, 6358–6366.
[12] J. Hildebrandt, N. Häfner, D. Kritsch, H. Görls, M. Dürst, I. B. Runnebaum, W. Weigand, *Int. J. Mol. Sci.* **2022**, *23*, 4976.
[13] C. Mügge, R. Liu, H. Görls, C. Gabbiani, E. Michelucci, N. Rüdiger, J. H. Clement, L. Messori, W. Weigand, *Dalton Trans.* **2014**, *43*, 3072–3086.
[14] C. Mügge, T. Marzo, L. Massai, J. Hildebrandt, G. Ferraro, P. Rivera-Fuentes, N. Metzler-Nolte, A. Merlino, L. Messori, W. Weigand, *Inorg. Chem.* **2015**, *54*, 8560–8570.
[15] J. Hildebrandt, N. Häfner, H. Görls, D. Kritsch, G. Ferraro, M. Dürst, I. B. Runnebaum, A. Merlino, W. Weigand, *Dalton Trans.* **2016**, *45*, 18876–18891.
[16] J. Hildebrandt, H. Görls, N. Häfner, G. Ferraro, M. Dürst, I. B. Runnebaum, W. Weigand, A. Merlino, *Dalton Trans.* **2016**, *45*, 12283–12287.
[17] J. Hildebrandt, N. Häfner, H. Görls, M.-C. Barth, M. Dürst, I. B. Runnebaum, W. Weigand, *Int. J. Mol. Sci.* **2022**, *23*, 6669.
[18] L. Tabrizi, B. Zouchoune, A. Zaiter, *RSC Adv.* **2019**, *9*, 287–300.
[19] B. Lippert, *Cisplatin: chemistry and biochemistry of a leading anticancer drug*, Verlag Helv. Chim. Acta, Zürich, **1999**, https://doi.org/10.1002/9783906390420.
[20] J. Reedijk, *Eur. J. Inorg. Chem.* **2009**, *2009*, 1303–1312.
[21] M. D. Hall, M. Okabe, D. W. Shen, X. J. Liang, M. M. Gottesman, *Annu. Rev. Pharmacol. Toxicol.* **2008**, *48*, 495–535.
[22] Y. Wang, J. Lv, X. Ma, D. Wang, H. Ma, Y. Chang, G. Nie, L. Jia, X. Duan, X.-J. Liang, *Curr. Drug Metab.* **2010**, *11*, 507–515.
[23] D.-w. Shen, I. Pastan, M. M. Gottesman, *Cancer Res.* **1998**, *58*, 268–275.
[24] Z. Guo, P. J. Sadler, *Angew. Chem. Int. Ed.* **1999**, *38*, 1512–1531; *Angew. Chem.* **1999**, *111*, 1610–1630.
[25] G. M. Mavligit, A. A. Zukwiski, L. M. Ellis, V. P. Chuang, S. Wallace, *Cancer* **1995**, *75*, 2083–2088.
[26] I. Kostova, *Recent Patents on Anti-Cancer Drug Discovery* **2006**, *1*, 1–22.
[27] H. P. Varbanov, S. M. Valiahdi, C. R. Kowol, M. A. Jakupec, M. Galanski, B. K. Keppler, *Dalton Trans.* **2012**, *41*, 14404–14415.
[28] J. Zhao, S. Gou, Y. Sun, L. Fang, Z. Wang, *Inorg. Chem.* **2012**, *51*, 10317–10324.
[29] A. Thuillier, J. Vialle, *Bull. Soc. Chim. Fr.* **1962**, 2182–2186.
[30] G. Singh, S. S. Bhattacharjee, H. Ila, H. Junjappa, *Synthesis* **1982**, *1982*, 693–694.
[31] H. Junjappa, H. Ila, *PCT Int. Appl.* **2004**, 2004101530.
[32] P. Kapoor, K. Lövqvist, Å. Oskarsson, *J. Mol. Struct.* **1998**, *470*, 39–47.
[33] C. K. Jorgensen, *Inorg. Chem.* **1964**, *3*, 1201–1202.
[34] R. G. Pearson, *Inorg. Chem.* **1973**, *12*, 712–713.
[35] M. K. Farh, F. V. Gruschwitz, N. Ziegenbalg, H. Abul-Futouh, H. Görls, W. Weigand, J. C. Brendel, *Macromol. Rapid Commun.* **2022**, 2200428.
[36] R. Saumweber, C. Robl, W. Weigand, *Inorganica Chim. Acta* **1998**, *269*, 83–90.
[37] K. Schubert, R. Saumweber, H. Görls, W. Weigand, *Z. Anorg. Allg. Chem.* **2003**, *629*, 2091–2096.
[38] K. Schubert, T. Alpermann, T. Niksch, H. Görls, W. Weigand, *Z. Anorg. Allg. Chem.* **2006**, *632*, 1033–1042.
[39] K. Schubert, H. Görls, W. Weigand, *Z. Naturforsch. B* **2007**, *62*, 475–482.

[40] G. R. Fulmer, A. J. M. Miller, N. H. Sherden, H. E. Gottlieb, A. Nudelman, B. M. Stoltz, J. E. Bercaw, K. I. Goldberg, *Organometallics* **2010**, *29*, 2176–2179.
[41] M. Kazemnejadi, A. Shakeri, M. Nikookar, R. Shademani, M. Mohammadi, *R. Soc. Open Sci.* **2018**, *5*, 171541.
[42] D. Nieto, A. M. González-Vadillo, S. Bruña, C. J. Pastor, C. Ríos-Luci, L. G. León, J. M. Padrón, C. Navarro-Ranninger, I. Cuadrado, *Dalton Trans.* **2012**, *41*, 432–441.
[43] C. López, A. Caubet, S. Pérez, X. Solans, M. Font-Bardía, E. Molins, *Eur. J. Inorg. Chem.* **2006**, *2006*, 3974–3984.
[44] C. López, S. Pérez, X. Solans, M. Font-Bardía, T. Calvet, *New J. Chem.* **2010**, *34*, 676–685.
[45] D. Talancón, C. López, M. Font-Bardía, T. Calvet, J. Quirante, C. Calvis, R. Messeguer, R. Cortés, M. Cascante, L. Baldomà, J. Badia, *J. Inorg. Biochem.* **2013**, *118*, 1–12.
[46] R. Cortés, M. Tarrado-Castellarnau, D. Talancón, C. López, W. Link, D. Ruiz, J. J. Centelles, J. Quirante, M. Cascante, *Metallomics* **2014**, *6*, 622–633.
[47] A. M. J. Fichtinger-Schepman, J. L. Van der Veer, J. H. J. Den Hartog, P. H. M. Lohman, J. Reedijk, *Biochemistry* **1985**, *24*, 707–713.
[48] V. Brabec, O. Hrabina, J. Kasparkova, *Coord. Chem. Rev.* **2017**, *351*, 2–31.
[49] T. C. Johnstone, J. J. Wilson, S. J. Lippard, *Inorg. Chem.* **2013**, *52*, 12234–12249.

Manuscript received: October 31, 2022
Revised manuscript received: December 26, 2022
Accepted manuscript online: January 10, 2023

